AD-A083 913 NAVAL RESEARCH LAB WASHINGTON DC F/G 20/9
ACCURATE ANALYTIC APPROXIMATIONS AND NUMERICAL SOLUTIONS FOR TH--ETC(U)
FEB 80 J H ORENS
UNCLASSIFIED NRL-MR-4167 NL

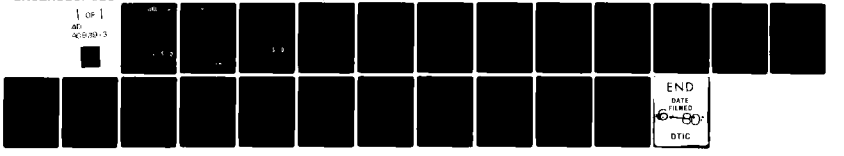

LEVEL II

12

NRL Memorandum Report 4167

SC

Accurate Analytic Approximations and Numerical Solutions for the Structure of Quasi-static Laser Driven Ablations Layers

JOSEPH H. ORENS

Laboratory for Computational Physics

February 29, 1980

NAVAL RESEARCH LABORATORY
Washington, D.C.

UNCLASSIFIED

SECURITY CLASSIFICATION OF THIS PAGE (When Data Entered)

REPORT DOCUMENTATION PAGE		READ INSTRUCTIONS BEFORE COMPLETING FORM
1. REPORT NUMBER NRL Memorandum Report 4167	2. GOVT ACCESSION NO. AD-A083 913	3. RECIPIENT'S CATALOG NUMBER
4. TITLE (and Subtitle) ACCURATE ANALYTIC APPROXIMATIONS AND NUMERICAL SOLUTIONS FOR THE STRUCTURE OF QUASI-STATIC LASER DRIVEN ABLATION LAYERS		5. TYPE OF REPORT & PERIOD COVERED Interim report on a continuing NRL problem. 6. PERFORMING ORG. REPORT NUMBER
7. AUTHOR(s) Joseph H. Orens		8. CONTRACT OR GRANT NUMBER(s)
9. PERFORMING ORGANIZATION NAME AND ADDRESS Laboratory for Computational Physics Naval Research Laboratory Washington, DC 20375		10. PROGRAM ELEMENT, PROJECT, TASK AREA & WORK UNIT NUMBERS NRL J.O. 62-0575-0-0 DOE Project No. NP010501
11. CONTROLLING OFFICE NAME AND ADDRESS		12. REPORT DATE February 29, 1980 13. NUMBER OF PAGES 22
14. MONITORING AGENCY NAME & ADDRESS(if different from Controlling Office)		15. SECURITY CLASS. (of this report) UNCLASSIFIED 15a. DECLASSIFICATION/DOWNGRADING SCHEDULE

16. DISTRIBUTION STATEMENT (of this Report)

Approved for public release; distribution unlimited.

17. DISTRIBUTION STATEMENT (of the abstract entered in Block 20, if different from Report)

18. SUPPLEMENTARY NOTES

This work was supported by the U.S. Department of Energy under Project No. NP010501.

19. KEY WORDS (Continue on reverse side if necessary and identify by block number)

Laser driven ablation layers
Equilibrium ablation models
Accelerating foils
Accelerating shells
Rayleigh-Taylor stability

20. ABSTRACT (Continue on reverse side if necessary and identify by block number)

Time dependent simulations of a laser driven accelerating shell and ablation layer have shown the presence of long lived "quasi-static" density and pressure profiles. This paper models the equilibrium solutions for a laser ablation layer both analytically and numerically and develops a detailed understanding of the nature of this flow. Such a model enables the calculation of the quantitative dependence of the shell thickness and acceleration, the peak density, velocity, and temperature of the shell, the width of the Rayleigh-Taylor region, and the distance to the critical surface on the total plasma mass, the critical density, and the absorbed and reflected laser flow

DD FORM 1 JAN 73 1473 EDITION OF 1 NOV 65 IS OBSOLETE
S/N 0102-014-6601

UNCLASSIFIED
SECURITY CLASSIFICATION OF THIS PAGE (When Data Entered)

CONTENTS

I. INTRODUCTION 1

II. STRUCTURE OF THE ACCELERATING SHELL AND BLOWOFF PLASMA 1

a. The Region of the Accelerating Shell ($\xi < 0$) 4
b. The Vicinity of the Density Peak ($\xi \approx 0$) 7
c. The Region of the Blowoff Plasma ($\xi \approx 0$) 8

III. NUMERICAL RESULTS 16

IV. CONCLUSIONS 17

REFERENCES 18

ACCURATE ANALYTIC APPROXIMATIONS AND NUMERICAL SOLUTIONS FOR THE STRUCTURE OF QUASI-STATIC LASER DRIVEN ABLATION

I. INTRODUCTION

Previous numerical simulations at NRL have shown that density and pressure profiles for an accelerating D-T shell and ablation layer can be temporally superimposed with very little scatter. Because of the presence of these long lived "quasi-static" profiles, we felt that it was important to model the equilibrium solutions for a laser ablation layer both analytically and numerically and to develop a detailed understanding of the nature of this flow. Facility with such a model enables us to calculate the quantitative dependence of the shell thickness and acceleration, the peak density, velocity, and temperature of the shell, the width of the Rayleigh-Taylor unstable region, and the distance to the critical surface on the total plasma mass, the critical density, and the absorbed and reflected laser flux. This "quasi-equilibrium", as determined by the input parameters of the configuration, can be used as an inexpensive input or driver for other numerical studies and as an equilibrium solution for stability analyses. Following is the detailed description of the laser ablation layer included in the numerical model.

II. STRUCTURE OF THE ACCELERATING SHELL AND BLOWOFF PLASMA

For our analyses we use the basic one-dimensional steady state fluid equations for a plasma slab transformed into an accelerating frame of reference

$$\text{continuity: } \frac{d}{dx}(\rho v) = 0 \tag{1a}$$

Manuscript submitted December 20, 1979.

$$\text{momentum: } \frac{d}{dx}(\rho v^2 + P) = \rho g - \left[\frac{I_a + 2I_r}{c}\right]\delta(x - x_c) \tag{1b}$$

$$\text{energy: } \frac{d}{dx}(Pv + Ev + q) = \rho g v + I_a\,\delta(x - x_c) \tag{1c}$$

where $\tau \equiv T/m_i$, $P = \rho\tau$, $E = \frac{1}{2}(3P + \rho v^2)$, $q = -Km_i^{7/2}\tau^{5/2}\frac{d\tau}{dx}$, and g is the acceleration of the slab. I_a is the absorbed laser flux, I_r is the reflected laser flux, and x_c is the location of the critical surface. As is evident, we are treating the plasma as a fluid with a γ of 5/3 and a classical plasma heat conductivity with a coefficient variation of $T^{5/2}$. The laser deposition is represented as a δ-function at the critical surface. Note that equation (1a) tells us that ρv = constant. To facilitate the analysis it is convenient to transform the basic equations (1), except at the critical surface, into a dimensionless form where the normalization variables, subscript 0, are those defined at the point of maximum density in the plasma slab.

$$\frac{d\beta}{d\zeta} = \frac{N_o}{2}\frac{1}{\beta^{5/2}}\left[5(\beta - 1) + M_o^2(\eta - 1) - 2\zeta\right] + \frac{1}{\beta^{5/2}} \tag{2a}$$

$$\frac{d\eta}{d\zeta} = -\frac{2\eta\left[\frac{d\beta}{d\zeta} - 1\right]}{M_o^2\eta - \beta} \tag{2b}$$

or

$$\frac{2}{N_o}\frac{d}{d\zeta}\left[\beta^{5/2}\frac{d\beta}{d\zeta}\right] = \beta\frac{d}{d\zeta}\ln(\eta\beta^3). \tag{2c}$$

The dimensionless variables are

$$\beta(\zeta) = \tau/\tau_o, \quad \eta(\zeta) = (\rho_o/\rho)^2, \quad \zeta = g/\tau_o\, x, \tag{3}$$

and the dimensionless coefficients are

$$N_o = \frac{\rho_o v_o}{km_i^{7/2} g\tau_o^{3/2}} \text{ and } \quad M_o^2 = v_o^2/\tau_o. \tag{4}$$

The isothermal mach number is defined by

$$M^2 \equiv \frac{v^2}{\tau} = \left(\frac{\rho_o}{\rho}\right)^2 \frac{v_o^2}{\tau} = \frac{\eta M_o^2}{\beta} \tag{5}$$

Only two of the three equations (2) are independent. Depending on the circumstances, we found that various pairs of the three equations were more convenient to analyze than others. Under this transformation the problem was reduced to solving for two dependent, dimensionless variables β (the temperature) and η (the density) based on one independent spatial variable ζ and two dimensionless coefficients N_o (primarily the thermal conductivity usually a large number), and M_o (the isothermal mach number at the density peak, usually a small number). We utilized this dimensionless set of equations (2) to generate either general numerical or analytic solutions and then matched these solutions to the specific physical constraints and boundary conditions to determine the desired self-consistent profiles. The numerical solutions were obtained by a Runge-Kutta integration of the non-linear coupled set of differential equations (2) while the analytic solutions were obtained by making appropriate approximations to the equations in the various regions and then solving the simplified set.

For the purpose of obtaining general analytic solutions, the set of equations (2) is conveniently divided into three regions. The first region is the accelerating shell ($\zeta < 0$). the second region is the vicinity of the density peak ($\zeta \approx 0$), and the third region is the blowoff plasma ($\zeta > 0$). Because of certain basic physical trends for the solutions β and η in each of these regions, it is possible to make simplifying assumptions that allow analytic solutions to the equations (2). As will be discussed later, there are other admissible solutions to these equations with counterintuitive physical trends but as yet these have not been sufficiently investigated to determine whether they, too are physically real.

a. The Region of the Accelerating Shell ($\zeta < 0$)

Rewriting equation (2a) into a more convenient form we find that:

$$5(\beta-1) + M_o^2(\eta-1) - 2\zeta = \frac{2}{N_o}\left[\beta^{5/2}\frac{d\beta}{d\zeta} - 1\right]. \tag{6}$$

The traditional physical profiles for this region require that $\frac{d\eta}{d\zeta} \leqslant 0$, $\beta \leqslant 1$, and $\eta M_o^2 \leqslant \beta$. In words, the density and temperature should decrease away from the density maximum at $\zeta = 0$ toward the inner regions of the accelerating shell ($\zeta < 0$), and for this region the flow is isothermally subsonic. Therefore from (2b) $\frac{d\beta}{d\zeta} \leqslant 1$ and correspondingly

$$0 \leqslant \beta^{5/2}\frac{d\beta}{d\zeta} \leqslant 1. \tag{7}$$

From (6) and (7) we then obtain the following two inequalities

$$5(\beta-1) + M_o^2(\eta-1) - 2\zeta \leqslant 0 \tag{8a}$$

and

$$5(\beta-1) + M_o^2(\eta-1) - 2\zeta + \frac{2}{N_o} > 0. \tag{8b}$$

Except for a very narrow region where $|\zeta| \approx \frac{1}{N_o}$ (N_o is usually large), Eqs. (8a) and (8b) imply that

$$5(\beta-1) + M_o^2(\eta-1) - 2\zeta \approx 0 \tag{9}$$

is quite a good approximation. By differentiating (2a) we find that

$$5\frac{d\beta}{d\zeta} + M_o^2\frac{d\eta}{d\zeta} - 2 = \frac{2}{N_o}\frac{d}{d\zeta}\left[\beta^{5/2}\frac{d\beta}{d\zeta}\right]. \tag{10}$$

Again, except where $|\zeta|$ is on the order of $\frac{1}{N_o}$ and $\beta^{5/2}\frac{d\beta}{d\zeta}$ is varying rapidly, we have the approximation that

$$5\frac{d\beta}{d\zeta} + M_o^2\frac{d\eta}{d\zeta} - 2 \approx 0. \tag{11}$$

Combining Eqs. (2b) and (11) gives us the further approximation that

$$\frac{d}{d\zeta}(\eta\beta^3) \approx 0 \tag{12a}$$

or

$$\eta\beta^3 \approx 1. \tag{12b}$$

This latter result can also be obtained from equation (2c).

Collecting our results, we have as a general approximate solution to the set of equations (2) for the region $\zeta < 0$,

$$5(\beta-1) + M_o^2(\eta-1) - 2\zeta \approx 0 \tag{13a}$$

$$\eta\beta^3 \approx 1. \tag{13b}$$

It is interesting to note that this approximation is independent of N_o and therefore the flow and profiles in the accelerating shell are not basically governed by thermal conductivity. Also equation (13b) states that the entropy P/ρ^γ is approximately constant throughout the accelerating shell which behaves like an adiabatic gas.

From equation (13b) we obtain

$$\frac{d\eta}{d\zeta} \approx -\frac{3}{\beta^4}\frac{d\beta}{d\zeta}. \tag{14}$$

Combining this result with equation (11) yields

$$\frac{d\beta}{d\zeta} \approx \frac{2\beta^4}{5\beta^4 - 3M_o^2}. \tag{15}$$

It is important to note that equation (15) does not hold when $\zeta = 0$ and $\frac{d\beta}{d\zeta} = 1$ $\left[\zeta = 0 \text{ is the turning point for the density. There } \frac{d\eta}{d\zeta}\Big|_{\zeta=0} = 0 \text{ and from (2b) } \frac{d\beta}{d\zeta}\Big|_{\zeta=0} = 1\right]$. Therefore it is evident that $\frac{d\beta}{d\zeta}$ varies from 1 to approximately $\frac{2}{5 - 3M_o^2}$ very quickly over a narrow region.

It is possible for the flow to approach an isothermal sonic point ($M_o^2\,\eta = \beta$) in this region. From (13a) and (13b) this occurs when

$$\beta(\zeta_s) \approx \sqrt{M_o} \tag{16a}$$

and

$$\zeta_s \approx 3\sqrt{M_o} - \frac{5 + M_o^2}{2}. \tag{16b}$$

Substituting (16a) into (15), we have

$$\frac{d\beta}{d\zeta}\Big|_{\zeta = \zeta_s} \approx 1 \tag{17}$$

where ζ_s is the location of the isothermal sonic point. This is an important result. It implies that equation (2b) may not be singular at the isothermal sonic point. In fact, from (14) we expect that

$$\frac{d\eta}{d\zeta}\Big|_{\zeta = \zeta_s} \approx -\frac{3}{M_o^2}.$$

Applying L'Hospital's rule to the full set of equations (2) in the limit where $\beta \to M_o^2\eta$ and $\frac{d\beta}{d\zeta} \to 1$ yields:

$$\lim_{\substack{\beta \to M_o^2 \eta \\ \frac{d\beta}{d\zeta} \to 1}} \frac{d\eta}{d\zeta} = -\frac{\left(\frac{N_o}{\beta^{3/2}} - 1\right)}{2M_o^2}\left[1 - \left[1 - \frac{4\left(\frac{3N_o}{\beta^{3/2}} - 5\right)}{\left(\frac{N_o}{\beta^{3/2}} - 1\right)^2}\right]^{1/2}\right]. \tag{18}$$

Since $\frac{N_o}{\beta^{3/2}} >> 1$ generally, Equation (18) tells us that

$$\left.\frac{d\eta}{d\zeta}\right|_{\zeta \to \zeta_s} \to -\frac{3}{M_o^2} \tag{19}$$

as expected. The fact that the flow approaches a well behaved, continuous isothermal sonic point is very helpful since it gives us a convenient position to define as the inner edge of the accelerating shell. This definition is reasonable since no physical information about the flow could be transmitted across this point.

b. The Vicinity of the Density Peak ($\zeta \approx 0$)

The simplest approach to determining an analytic approximation in this region is to expand the system of equations (2) in a Taylor series about $\zeta = 0$. Doing this for small ζ yields to third order

$$\beta \approx 1 + \zeta + \frac{\zeta^2}{4}(3N_o - 5) + \frac{\zeta^3}{12}\left[\frac{N_o(3N_o-5)}{2}\left(\frac{5-3M_o^2}{1-M_o^2}\right) - 5(3N_o - 5) - \frac{15}{2}\right] \tag{20a}$$

and

$$\eta \approx 1 + \frac{\zeta^2/2}{1-M_o^2}(3N_o - 5) + \frac{\zeta^3/6}{1-M_o^2}\left[\frac{N_o(3N_o-5)}{2}\left(\frac{5-3M_o^2}{1-M_o^2}\right) - (3N_o - 5)\left(\frac{7-5M_o^2}{1-M_o^2}\right) - \frac{15}{2}\right]. \tag{20b}$$

Since $\zeta = 0$ is to be a density maximum

$$\left.\frac{d^2\eta}{d\zeta^2}\right|_{\zeta=0} > 0 \tag{21}$$

which by differentiating equation (20b) twice yields

$$N_o > \frac{5}{3}. \tag{22}$$

This is not a very stringent criteria for N_o. Generally for physical problems of interest $N_o >> 5/3$. It is also important to note that the region where the Taylor expansions (20) are accurate is exceedingly narrow. Trying to utilize these results for even a distance on the order of the thickness of the ablation layer does not yield valid results. In fact, equations (2) are included more for completeness than for their practical importance.

c. The Region of the Blowoff Plasma ($\zeta > 0$).

Two very important regions lie in the blowoff. The first is the Rayleigh-Taylor unstable region where the gradients of density and pressure have opposite sign. The second is the vicinity of the critical surface where the laser deposition occurs. In this region $\frac{d\beta}{d\zeta}$ is increasing rapidly from its value of 1 at $\zeta = 0$. Corresponding, $\beta >> 1$ except very near the density peak. It is expected that this region be isothermally subsonic at least until the critical surface is reached. Therefore,

$$| M_o^2(\eta - 1) - 2\zeta | << 5(\beta - 1) \tag{23}$$

is a valid approximation except in a very narrow region about $\zeta = 0$ where it is in error by about 40%. Here retaining ζ is important and the approximation is more properly written as

$$M_o^2(\eta - 1) << 5(\beta - 1) - 2\zeta. \tag{24}$$

The error in (23) potentially could be as great as 20% in the vicinity of the critical surface as well. In practice (numerical integrations) it never becomes that large. Under these approximations equation (2a) becomes either

$$\frac{d\beta}{d\zeta} \approx \frac{N_o}{2}\,\frac{5}{\beta^{5/2}}\left[\beta - \left[1 - \frac{2}{5N_o}\right] - \frac{2}{5}\,\zeta\right]. \tag{25a}$$

or

$$\frac{d\beta}{d\zeta} \approx \frac{N_o}{2}\,\frac{5}{\beta^{5/2}}\left[\beta - \left[1 - \frac{2}{5N_o}\right]\right] \tag{25b}$$

Equation (25b) can be solved analytically to yield:

$$\zeta = \frac{4}{5N_o}\left[\frac{1}{5}\left(\beta^{5/2}-1\right) + \frac{\left[1-\frac{2}{5N_o}\right]}{3}\left(\beta^{3/2}-1\right) + \left[1-\frac{2}{5N_o}\right]\left(\beta^{1/2}-1\right)\right.$$

$$\left. - \frac{1}{2}\left[1-\frac{2}{5N_o}\right]^{5/2} ln\left[\frac{\beta^{1/2}+\sqrt{1-\frac{2}{5N_o}}}{1+\sqrt{1-\frac{2}{5N_o}}}\;\frac{1-\sqrt{1-\frac{2}{5N_o}}}{\beta^{1/2}-\sqrt{1-\frac{2}{5N_o}}}\right]\right]. \tag{26}$$

Equation (25a) can also be solved analytically to yield an approximation near $\zeta = 0$ that is more exact than (26), but little is gained by including it here due to its complexity. Though it is not crucial to use this more exact approximation to define the Rayleigh-Taylor unstable region, its use does improve the results in a measurable way. For $\zeta > 0$ it is advantageous to write equation (2b) in terms of the pressure where

$$\frac{P}{P_o} = \frac{\beta}{\sqrt{\eta}}. \tag{27}$$

This gives two interesting forms

$$\frac{d}{d\zeta}\left[ln\ \frac{\eta}{\beta^2}\right] = -2\frac{d}{d\zeta}\left[ln\ P/P_o\right] = \frac{1}{\beta}\ \frac{d}{d\zeta}\ (M_o^2\ \eta - 2\zeta) \tag{28a}$$

and

$$2\frac{d}{d\zeta}\left[\frac{\beta}{\sqrt{\eta}}\right] = 2\frac{d}{d\zeta}\left[P/P_o\right] = -\frac{1}{\sqrt{\eta}}\ \frac{d}{d\zeta}\ (M_o^2\ \eta - 2\zeta). \tag{28b}$$

Adding (28b) to (28a) yields

$$\frac{d}{d\zeta}\left[ln\ \frac{\eta}{\beta^2}\right] = \frac{d}{d\zeta}\left\{[2\beta + M_o^2(\eta-1) - 2\zeta]\left[\frac{1}{\beta} - \frac{1}{\sqrt{\eta}}\right]\right\} - [M_o^2(\eta-1) - 2\zeta]\ \frac{d}{d\zeta}\left[\frac{1}{\beta} - \frac{1}{\sqrt{\eta}}\right] \tag{29}$$

The second term on the R.H.S. of (29) is effectively a coefficient times the rate of change of the pressure. Conveniently it turns out that the rate of change of the pressure is significant where the coefficient is small and the coefficient is significant where the rate of change of the pressure is small. Therefore the term is always small and may be neglected.

We obtain as an approximation

$$\frac{\eta - \beta^2 \exp\left\{[2\beta + M_o^2(\eta-1) - 2\zeta]\left[\frac{1}{\beta} - \frac{1}{\sqrt{\eta}}\right]\right\}}{\eta - \beta^2} = 0. \tag{30}$$

The presence of $\eta - \beta^2$ in the denominator compensates for the additional root at $\eta = \beta^2$ introduced by adding (28b) to (28a). Equations (26) and (30) are then an extremely good approximation to the general solution for $\zeta > 0$. It is also relevant to note that these analytic solutions with the modifications included due to (25a) will hold around $\zeta \approx 0$ and even be valid when ζ is slightly less than zero and $\beta^{5/2}\ \frac{d\beta}{d\zeta}$ is varying rapidly as noted earlier.

From (28b) we obtain two interesting results. First

$$\frac{d}{d\zeta}\left[P/P_o\right]\Big|_{\zeta=0} = 1 \tag{31}$$

and second

$$\frac{d}{d\zeta}\left[P/P_o\right] = 0 \text{ when } \frac{d\eta}{d\zeta} = \frac{2}{M_o^2}. \tag{32}$$

Combining (32) and (2b) yields

$$\frac{d}{d\zeta}\left[P/P_o\right] = 0 \text{ when } \frac{d\beta}{d\zeta} = \frac{\beta}{M_o^2\eta} \tag{33}$$

or from (5)

$$\frac{d}{d\zeta}\left[P/P_o\right] = 0 \text{ when } M^2\frac{d\beta}{d\zeta} = 1. \tag{34}$$

Equations (32) and (33) or (34) give us respectively the rate of change of the density and the temperature at the turning point of the pressure. It is just this offset of the density and pressure peaks that bounds the Rayleigh-Taylor unstable region, so-called because density and pressure gradients are opposed.

Combining (33) with equation (2a) yields an equation defining the relationship of the variables at the pressure peak

$$\frac{\beta}{M_o^2\eta} = \frac{N_o}{2}\frac{1}{\beta^{5/2}}\left[5(\beta-1)+\frac{2}{N_o}+M_o^2(\eta-1)-2\zeta\right]. \tag{35}$$

The relevant question is whether equation (35) has a solution for all values of M_o and N_o. From Eq. (32), in the Rayleigh-Taylor unstable region

$$0 \leqslant \frac{d\eta}{d\zeta} \leqslant \frac{2}{M_o^2}. \tag{36}$$

Therefore

$$\frac{d}{d\zeta}\left[M_o^2(\eta-1)-2\zeta\right] \leqslant 0 \quad \text{or} \quad M_o^2(\eta-1)-2\zeta \leqslant 0 \tag{37}$$

there applying (37) to equation (35) we obtain the condition for the existence of a pressure peak not located at $\zeta = 0$,

$$\beta < \frac{N_o}{2}\,\frac{M_o^2\eta}{\beta^{5/2}}\left[5(\beta-1)+\frac{2}{N_o}\right] \tag{38}$$

also in the Rayleigh-Taylor region

$$\frac{d}{d\zeta}\left[P/P_o\right] \geqslant 0 \quad \text{or} \quad \frac{P}{P_o} \geqslant 1 \tag{39}$$

or from equation (27)

$$\eta \leqslant \beta^2. \tag{40}$$

Combining inequalities (38) and (40) requires at the pressure peak

$$\beta^{3/2} < \frac{N_o}{2}\,M_o^2\left[5(\beta-1)+\frac{2}{N_o}\right]. \tag{41}$$

It is tedious, but straightforward to show that there can be no regime where $\beta - 1 \geqslant 0$ and inequality (41) can hold when

$$N_o M_o^2 \leqslant \frac{2}{5}\sqrt{3}. \tag{42}$$

This is a rather significant result since it shows that not all values of M_o and N_o are admissible if one requires a solution to the set of equations (2) where there is a turning point in the pressure profile. Figure 1 displays graphically the allowable region of $M_o - N_o$ space.

The only other important modeling necessary for the region $\zeta > 0$ is near the critical surface. Here we integrate equations (1) across the critical surface to obtain the jump conditions and utilize the density shelf criteria of Felber[1] and *Lee at al.*[2] where

$$\sqrt{\eta_-} = 2\sqrt{\eta_c}\,\frac{(1-M_-)^2}{M_-^2 - \ln(M_-^2) - 1} \tag{43}$$

with the subscript minus referring to the values just interior to the jump and

$$\eta_c = \left(\frac{\rho_o}{\rho_c}\right)^2 \quad (\rho_c \textit{ is the critical density}). \tag{44}$$

We force the temperature to remain constant across the jump and the heat flux to be zero outside the critical surface. We did not believe that it was important to model the underdense gas outside the critical surface since the density is so low there. Felber[1] has chosen to model this region as an adiabatic gas and that would probably be as good a choice as any other. We do require that the flow out of the critical surface be supersonic and that gives us an additional constraint on M_o that

$$M_o^2 < M_-^2 < \frac{3}{5} \tag{45}$$

This constraint is also included in Figure 1. When M_o and N_o are chosen within the bounds depicted in Figure 1 the solutions to equations (2) are profiles that can be given physical explainations. For values outside that regime equations (2) are still solvable, but it is not clear whether the profiles generated also have a physical significance or are merely mathematical curiosities. This question is worthy of further investigation. There are two possible approaches to obtain profile solutions to equations (2) for given specific boundary conditions. First the coupled set of non-linear first order differential equations can be integrated numerically by a Runge-Kutta method and then the boundary conditions matched. Second, the general analytic approximations (13), (26), and (30) can be utilized instead of a numerical integration and then matched to the specific boundary condition. Conceptually there is not much difference in either method. Because of the complexity of the analytic approximations both methods require the use of a computer. The major advantage of the analytic approximation approach is that, by

allowing an error in the results of a few percent, significant computational time can be saved. Also the analytic approach often gives a better insight into what is physically occurring. The three available boundary conditions not previously taken into account are the total plasma mass, the absorbed laser flux, and the reflected laser flux. Certainly the original slab mass must be encompassed by the density profile. For our model we assume that all the mass lies between the interior isothermal sonic point and the critical surface. Because the densities outside this region are exceedingly small compared to the peak density, this approximation should have little effect on the results. Therefore, if m is the total slab mass per unit area,

$$m = \int_{x_s}^{x_c} \rho dx = \frac{\rho_o \tau_o}{g} \int_{\zeta_s}^{\zeta_c} \frac{1}{\sqrt{\eta}}\, d\zeta \tag{46}$$

or from (4)

$$m = \frac{k m_i^{7/2}}{M_o} N_o \tau_o^2 \int_{\zeta_s}^{\zeta_c} \frac{1}{\sqrt{\eta}}\, d\zeta. \tag{47}$$

Evaluation of the integral in (46) or (47) follows from an integration of equation (28b)

$$\int_{\zeta_s}^{\zeta_c} \frac{1}{\sqrt{\eta}}\, d\zeta = \frac{\beta}{\sqrt{\eta}} + M_o^2 \sqrt{\eta} \Bigg|_{\zeta_s}^{\zeta_c} \tag{48a}$$

or

$$\int_{\zeta_s}^{\zeta_c} \frac{1}{\sqrt{\eta}}\, d\zeta = \frac{\beta_c}{\sqrt{\eta_c}} + M_o^2 \sqrt{\eta_c} - \left[\frac{\beta_s}{\sqrt{\eta_s}} + M_0^2 \sqrt{\eta_s}\right] \tag{48b}$$

and since $M_0^2\, \eta_s = \beta_s$

$$\int_{\zeta_s}^{\zeta_c} \frac{1}{\sqrt{\eta}} d\zeta = \frac{\beta_c}{\sqrt{\eta_c}} + M_o^2 \sqrt{\eta_c} - 2M_0^2 \sqrt{\eta_s} \tag{49a}$$

or

$$\int_{\zeta_s}^{\zeta_c} \frac{1}{\sqrt{\eta}}\, d\zeta = \frac{\beta_c}{\sqrt{\eta_c}} + M_o^2 \sqrt{\eta_c} - 2M_o \sqrt{\beta_s}\,. \tag{49b}$$

Applying the approximations (16)

$$\int_{\zeta_-}^{\zeta_c} \frac{1}{\sqrt{\eta}} d\zeta \approx \frac{\beta_c}{\sqrt{\eta_c}} + M_o^2 \sqrt{\eta_c} - 2M_o^{5/4} \tag{50}$$

Of course, in (50) η_c and β_c are, as yet, an undetermined parameters.

At the critical surface we handle the jump conditions and laser deposition much as Felber[1] did where

$$\phi^2 \equiv 1 + 2\frac{I_a - \Delta q}{\rho_- v_-^3} = 1 + 2\frac{I_a - \Delta q}{\rho_o M_o \tau_o^{3/2} \beta_c M_-^2} \tag{51}$$

and we have used the constancy of ρv, and equation (5). It is also true from reference 2 that

$$\frac{I_a + 2I_r}{c\rho_o \tau_o \beta_c} \sqrt{\eta_-} = (1 - M_-^2 \phi)\ (1 - \frac{1}{\phi}) \tag{52}$$

By use of equations (43), (47), (50), (51), and (52), we are able to determine the position of the critical surface for a given M_o and N_o. This is accomplished by beginning at $\zeta = 0$ and moving in the direction of increasing ζ using a Runge-Kutta solution of equations (2) or using the analytic approximations. At each point we assume that we have reached the critical surface. Then from (47) and (50) we can obtain the value τ_o such that all the plasma mass would be contained within the density profile to that point. With the τ_o equations (51) and (52) will determine the corresponding ρ_o. This value of ρ_o may then be used to see if equation (43) is satisfied. When (43) is satisfied, we have reached the critical surface. Also we have the values of ρ_o and τ_o needed to transform the general profiles into the specific profiles for the given boundary conditions. The other values of interest v_o and g can be found from (4).

The preceeding discussion has masked a rather curious fact. Even with all the criteria we have specified, we cannot determine a unique solution based on a single pair of M_o and N_o but rather have obtained a whole family of possible "quasi-equilibrium" solutions based on values of

M_o and N_o only constrained as in Figure 1. Maybe we have not specified all the available boundary conditions but it is difficult to think of another two, only based on the equilibrium, that we are at liberty to specify. More likely, what the results are telling us is that there really are various possible "quasi-equilibrium" states and just which one would occur in a given physical situation might be determined by the neccessarily time-dependent evolution leading up to that equilibrium. Such an effect might be an initial shock which impacts an entropy to the shell. Others may exist.

III. NUMERICAL RESULTS

Figure 2 displays the profiles of density, temperature, pressure, and isothermal mach number for the "quasi-equilibrium" where $Km_i^{7/2} = 10^{-33}$, $\rho_c = 4\times10^{-3}$ g/cm^3, $I_a = 10.2$ TW $/cm^2$, $I_r = 10.2 TW/cm^2$, $m = .773 mg/cm^2$ $M_o \approx .07$, and $N_o \approx 700$. These profiles were obtained by a Runge-Kutta integration of the equations (2), but curves generated through the analytic approximations discussed earlier are virtually indistinguishable. These are rather typical results and while variation of M_o and N_o, within the constraints of Figure 1, does change the profiles quantitatively there is not much qualitative variation. The density, temperature, and pressure are seen to decrease smoothly away from the density peak toward the isothermal sonic point. For this case the thickness of the shell is about 35 microns and the peak density is about $.3 g/cm^3$. The corresponding temperatures and pressures at the density peak are respectively approximately 8×10^{12} cm^2/sec^2 and 2.5×10^{12} $dyne/cm^2$. The acceleration for the shell is about 4×10^{15} cm/sec^2. It is impossible to see in the figure, but the offset of the pressure and density peaks is about .1 micron. The peak pressure is only slightly greater than the pressure at the density peak. In the blowoff plasma the density drops sharply while due to the thermal conductivity the temperature increases rapidly. It is interesting to note that the decrease in density

is nearly balanced by the increase in temperature such that the pressure remains relatively constant. The critical surface is approximately 100 microns from the density peak and the critical temperature is about 4.5×10^{14} cm^2/sec^2. The density and isothermal mach number just inside the critical surface are respectively approximately 4.5×10^3 g/cm^3 and .6. These profiles have been used as initial conditions for time varying models and are seen to remain relatively unchanged for long periods of time. Therefore they are truly "quasi-equilibrium" solutions. Further, since the density and pressure gradients in the constant adiabat shell are aligned, the shell interior is Rayleigh-Taylor stable.

IV. CONCLUSIONS

Development of this "steady-state" model is still continuing. The most important question yet to be resolved is how to choose M_0 and N_0. What is desired is to relate M_0 and N_0 to some physical properties that would remain constant for the solutions while external parameters like the plasma mass or the laser intensity are slowly varied. One such possibility is the entropy of the accelerating shell. We have utilized one of our "quasi-equilibrium" solutions as an initial condition to a time dependent simulation model and followed the burning of the shell. During the evolution, the shell entropy did remain relatively constant. We have also examined the constancy of the shell momentum, but, as yet, have not reached any definite conclusions.

Our model has been used as an initializer to time dependent ablation models and as a pressure driver for a laser-target compression simulation. For this latter case the "steady-state" model was used to relate the variation of the laser intensity to the pressure at the surface of the shell. Generally we used the analytic approximations for these studies, since it entails a vast savings in computational time. We also plan to utilize our model as an equilibrium for a piggy-back analysis of Rayleigh-Taylor stability in the ablation layer plasma.

REFERENCES

1. F.S. Felber, "Steady-State Model of a Flat Laser-Driven Target," *Phys. Rev. Lett. 39*, 84 (1977).

2. K. Lee, D.W. Forslund, J.M. Kindel, and E.L. Lindman, "Theoretical Derivation of Laser Induced Plasma Profiles," *Phys. Fluids 20*, 51 (1977).

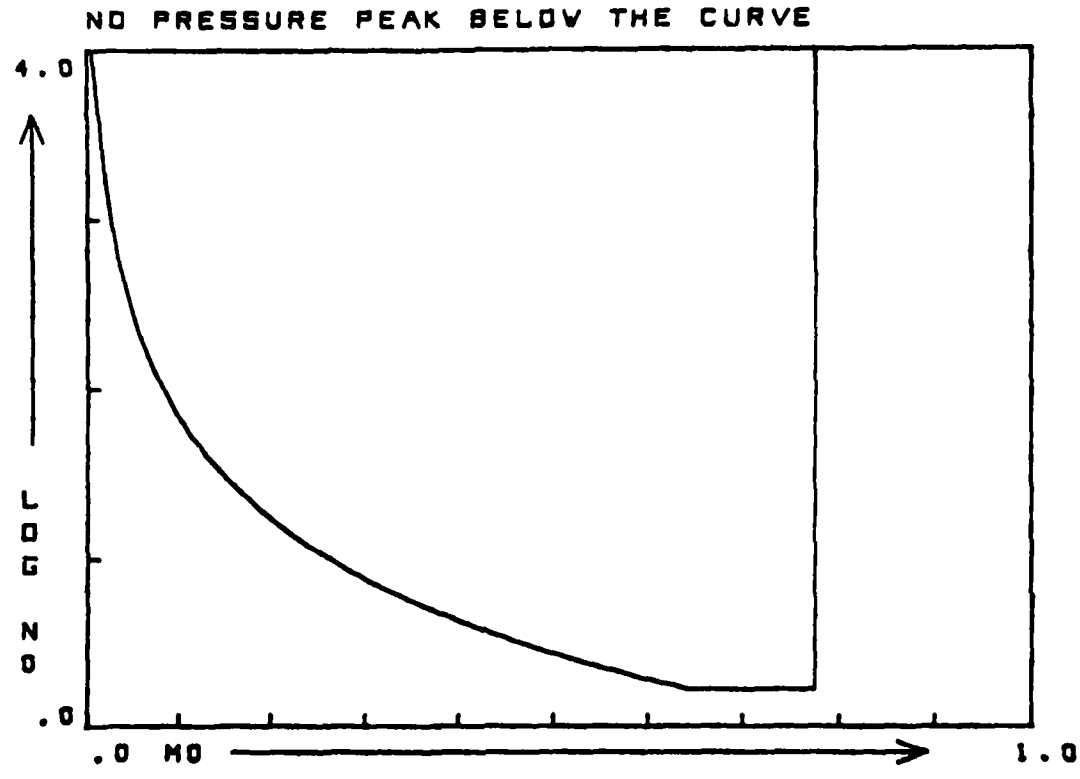

Fig. 1 — The region of $M_0 - N_0$ space that yields physically intuitive solutions. For the region below the curve there is no turning point in the pressure profile. For the region to the right of the curve the flow out of the critical surface is not supersonic.

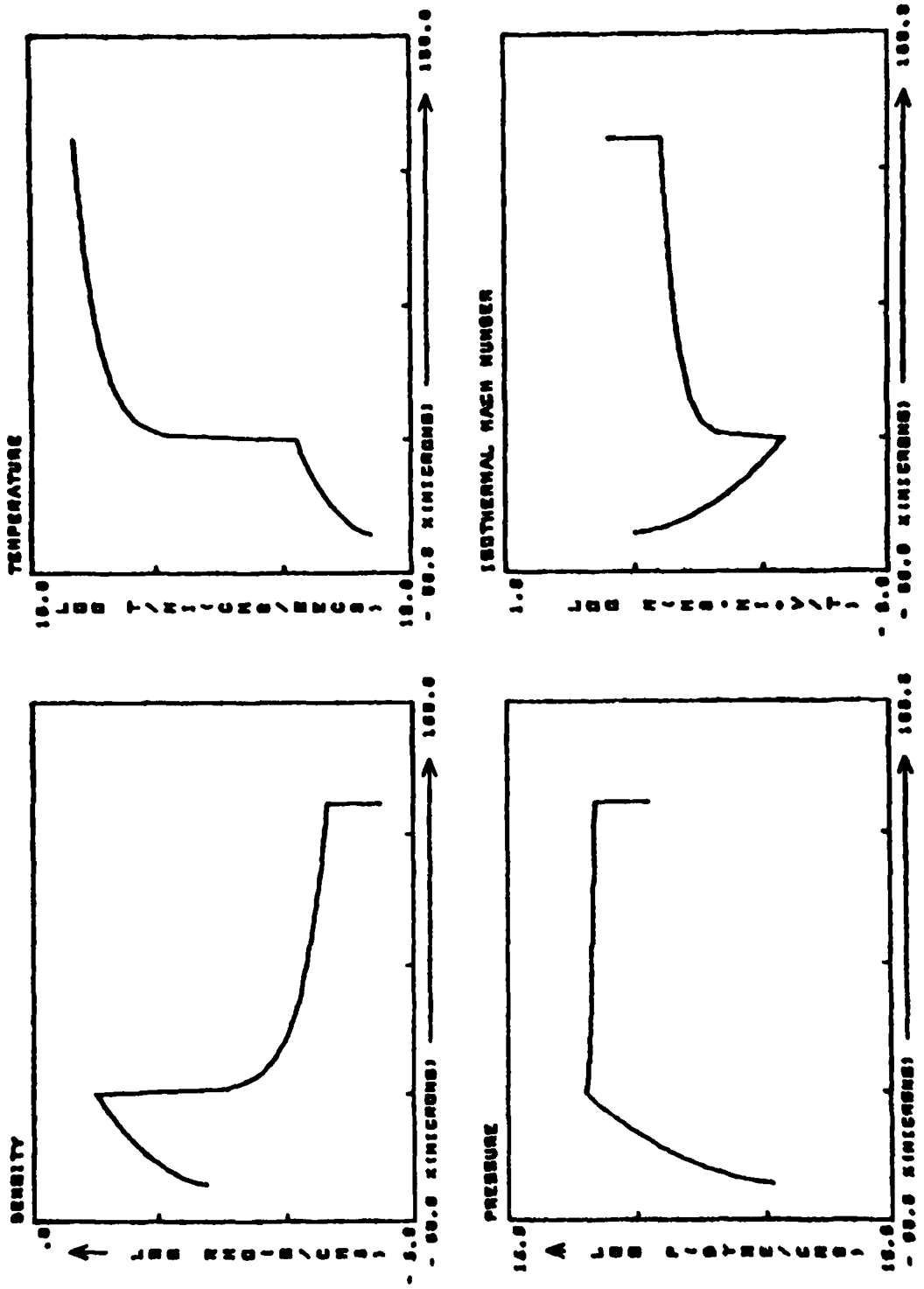

Fig. 2 — Typical solution profiles. Results are for the case where $Km_i^{7/2} = 10^{-33}$, $\rho_c = 4 \times 10^{-3}$ g/cm, $I_a = 10.2$ TW/cm^2, $I_r = 10.2$ TW/cm^2, m = .773 mg/cm^2, $M_0 \approx .07$, and $N_0 \approx 700$.